Materials International
Open Access Journal (ISSN: 2668-5728)

Article
Volume 6, Issue 4, 2024, 39
https://doi.org/10.33263/Materials64.039

Adsorption of Volatile Nor-Isoprenoid Ketone with Bovine Serum Albumin via Spectroscopic and Computational Investigation

Sankari Mohan [1,2], Hridya Hemachandran [3], Thirumal Kumar D [4], George Priya Doss C [1], Reshma Anjum M [2], G. Narasimha [5], Rossyda Priyadharshini [6], Veeranoot Nissapatorn [7], Siva Ramamoorthy [1,*]

1 School of BioSciences and Technology, VIT University, Vellore-632014
2 Sri Padmavathi Mahila Visvavidyalayam (Women's University), Tirupati
3 Muga Silkworm Seed Organisation, Central Silk Board, Guwahati, Assam
4 Meenakshi Academy of Higher Education and Research
5 Department of Virology, Sri Venkateshwara University, Tirupati
6 Universitas Pembangunan Nasional Veteran Jawa Timur, Indonesia
7 Walailak University, Thailand
* Correspondence: rsiva@vit.ac.in;

Scopus Author ID 16242802500
Received: 9.04.2024; Accepted: 6.10.2024; Published: 10.12.2024

Abstract: β- Ionone is a natural terpenoid compound exploited as a flavoring additive in food industries globally. β-Ionone is a vital compound of scent in the flowers of *Lawsonia inermis L.*, *Petunia hybrida*, and *Boronia megastigma*. One of the most popular flowers in China is sweet osmanthus, which is valued for its aroma and ornamental qualities. The current study analyzed the interlinkage of β-Ionone with bovine serum (BSA) by spectrofluorometry and circular dichroism supported by molecular modeling studies. A sturdy decline in the Stern-Volmer quenching constant with enhanced thermal reading exhibits the static quenching mechanism. The thermodynamic investigations, such as ΔH and ΔS values for the interaction of β-Ionone with BSA, were studied. The negative ΔH and the negative ΔS show that the binding process of β-Ionone with BSA was impulsive and the configuration of β-Ionone and BSA complex was exothermic. Further, we analyzed the fastening prototype using in silico tools such as Autodock and Protox servers. Based on our investigational results, we observed that the β-Ionone with BSA had a prominent binding affinity with -6.2 kcal/mol binding energy with no toxic effects. From our findings, we revealed that BSA with β-Ionone has a great impact upon interaction. From our results, β-Ionone has a higher binding affinity with protein, thus serving as an effective volatile food additive.

Keywords: β-ionone; spectrofluorometer; molecular modeling; binding affinity; bovine serum albumin.

1. Introduction

The volatile ketone, β-ionone, is an apocarotenoid that shapes the fundamental core configuration and is intermediate for all-trans-retinoic acid, Vitamin A1-alcohol, β-carotene, and Vitamin A. The word "ionone" is derived from the Greek words "iona" (violet), which alludes to the smell of violets, and "ketone," which relates to the ionone's chemical structure. Ionone is a monocyclic terpenoid ketone with a backbone of 13 carbon atoms. The cleavage product of -carotene at positions 9, 10, and 9′, 10′ is –ionone [1]. β-Ionone is a crucial component of scent in the flowers of *Lawsonia inermis L.* (henna), Petunia hybrida, and

Boronia megastigma (*Petunia megastigma*). One of the top ten most popular flowers in China is sweet osmanthus (*Osmanthus fragrans*), which is valued for both its aroma and its ornamental qualities. A significant portion of its aroma includes -ionone. Birds, bats, and insects are just a few pollinators visiting the blossoms of the mangrove plant, Nypa fruticans. The carotenoid derivatives -ionone, -ionone, dihydro-ionol, and -ionone make up the majority of the floral aroma chemistry of *N. fruticans*. These floral aromas could be a key element in luring pollinators. One of the volatile compounds found in the blooms of *Acacia farnesiana* is -ionone [1-3]. The attraction of pollinators may depend heavily on these floral smells. β-Ionone has been considered as GRAS by the USFDA, anticipating utility in food industries.

The predominant soluble protein in the blood is serum albumin, which serves as the transporter, distributor, and participant in the metabolism of various endogenous and foreign substances. It also maintains osmotic pressure. It is the essential serum component and offers particular binding sites for metals crucial for biological processes. Almost 76% sequence homology exists between human serum albumin and bovine serum albumin [4,5]. Based on structural similarity, we selected BSA as the model protein since it is the most prevalent protein in blood plasma. It serves various biological purposes, including fatty acids, amino acids, metals, hormones, medicines, and other substances for storage and transportation. BSA is commonly used to study the binding of bioactive compounds [6-8]. Several studies noted the development of complexes between BSA and other carotenoids like –carotene, astaxanthin with HSA and BSA, and crocin bixin with BSA through spectroscopically, thermodynamic methods and in silico approaches. Their findings showed that the processes leading to forming proteins/carotenoid complexes were both enthalpically and entropically driven [9-13].

Protein interaction with carotenoid and its derivatives is widely used to study the metabolism and transport of bioactive compounds. Numerous studies have been conducted on the molecular interactions with proteins, drugs, and some organic molecules [14-16]. Till now, no research has been done on BSA with β-ionone binding, even if it has medical significance. In this investigation, we report the interaction of β-Ionone with BSA using spectroscopic and binding studies, including binding parameters, quenching mechanism, and thermodynamic parameters such as enthalpy, entropy were discussed, and the fluorescent quenching results slight red shift indicating the interaction of β-Ionone induced hydrophilicity to the protein fluorophore. Besides, molecular docking was analyzed to expose the receptor site of the β-Ionone. The study pays the vital acquaintance for the binding mode towards the affinity of β-Ionone to protein. It is obliging for insights into its consequence on polypeptide function throughout the biological progression. Presumably, to our understanding, there is a lack of information on the interaction of β-Ionone with BSA.

2. Materials and Methods

2.1. Materials and solutions.

Analytical reagent grade was utilized for all compounds and reagents in this study. β-ionone was acquired from Sigma (St. Louis, MO, USA). Dimethyl sulfoxide (DMSO) and bovine serum albumin (BSA) were obtained from Himedia Laboratories, India. For β ionone solubilization, a 10% v/v concentration of DMSO was used. The water used to prepare the buffer solution was Milli-Q water (18.2 MΩ). BSA stock solution was prepared using 0.0l M phosphate buffer at pH 7.4, and the stock solution was made with care using 10% DMSO.

2.2. Spectral measurement.

The fluorescence spectra were recorded at various temperatures measured by a Hitachi F-7000 spectrofluorophotometer at a range of temperatures (298, 310, and 313K) in 1 cm quartz cell. The maximum excitation wavelength of BSA was 280 nm, and the maximum emission wavelength of BSA was 348 nm. 5nm was the final width of the emission and excitation slits. At an excitation wavelength of 290 nm, the steady concentration of 100 µM BSA in phosphate buffer was first determined to quantify the fluorescence quenching. A series of increasing concentrations of β ionone solutions from 1 to 10 µM was titrated, and a variable in fluorescent intensity was detected separately. Fluorescence quenching was plotted using the Stern-Volmer equation. Vant Hoff plots were used to analyze the thermodynamic parameters (ΔH and ΔS), and thermodynamic analysis was used to analyze the quenching constant at different temperatures. The three-dimensional fluorescence spectra of BSA alone, BSA: β ionone complex, was measured at the wavelength of 200 – 600 nm at 298K to state the conformational changes [11,17-20].

2.3. Circular dichroism spectroscopy.

The circular dichroism (CD) spectrum measurements were documented on the Jasco J-715 spectropolarimeter under constant nitrogen flush. The measurement was taken at 200-400nm at room temperature and conducted at pH 6.8. The CD spectra were measured with and without the presence of β-Ionone in phosphate buffer (pH 6.8). BSA spectrum (0.01 mg of BSA was dissolved in 0.1 M phosphate buffer, pH 7.4) was noted, to which an increasing concentration of β-ionone was added, and the spectrum was documented. Each spectrum was the mean of three runs at a 100 nm/min scan speed, 1.0 nm bandwidth, and 0.5 nm resolution. For phosphate buffer (pH 7.4), the entire detected CD spectral baseline was removed. Version 1 of the Jasco secondary structure appraisal software examined the secondary structural subjects of each scan [21-23].

2.4. Computational studies.

2.4.1. Molecular docking.

The 3D structures of the bovine serum albumin (BSA) and human serum albumin (HSA) were obtained from the Protein Data Bank (PDB) with the IDs 4F5S and 1AO6 [24]. The active sites of the proteins were obtained from the previous literature [11]. The canonical SMILES of Beta-ionone were retrieved from the PubChem database with CID 638014. This was converted to the 3D structure using an online Corina demo server. The molecular docking was performed using version 4.2 of the software AutoDock. Before analysis, the protein structures were refined by removing crystallographic water molecules and applying hydrogen in the perfect arrangement to the protein. The beta ionone's torsions were set. The files were saved in PDBQT file format, and the proteins' starting parameters and van der Waals were assigned a good depth of 0.100 kcal/mol. The active site's grid was established. The AutoDock tools were used to create docking parameter files (DPF) and grid parameter files (GPF). Finally, the Lamarckian Genetic Algorithm was used to produce potential binding conformations of protein-ligand. This gathered the binding energy in ten distinct positions. The complex was selected with the highest binding capacity for the visualization [25-28].

2.4.2. Molecular dynamics simulations.

BSA- β-Ionone and HSA- β-Ionone subjected to the molecular dynamics simulations (MDS). MDS were performed using the GROMACS package with the GROMOS96 43a1 force field. The parameters for the β-Ionone were obtained from the ATB online server. The topology of the structure was developed, and a cubic water box was constructed around it. To neutralize the whole setup, ions were added based on the charge. Energy minimization of 100 ps was carried out after the system was set up. Once the minimum energy was reached, for 100 ps each, the model was balanced with NVT and NPT analysis. Finally, for 10 ns, the whole proteins-beta iodine complexes were exposed to MDS. Each complex was subjected to RMSD, RMSF, and Gyration analysis after the MDS [29-31].

2.4.3. Toxicity prediction.

The β-ionone toxicity level was predicted using ProTox [32], and the pkCSM [33] server was used to recognize any harmful activity associated with the ligands. Input was used as canonical SMILES of b-ionone. Based on LD50 values, ProTox classifies ligands 1 through 6, with class 1 drugs being extremely toxic and class 6 drugs being safe. Only the toxicity analysis was employed in the current work to determine the nature of the ligands out of the several outputs that the pkCSM tool affords.

3. Results and Discussion

3.1. Fluorescence quenching spectra and mechanism.

A fluorescence spectrum was studied to investigate the interaction between β-Ionone and BSA. This technique extensively investigated molecular interactions, such as collisional quenching, excited-state reactions, ground-state complex forms, energy transfer between molecules, and substance-protein interactions. We examined the impact of temperature at various temperatures to research the quenching mechanism [34]. As said, there are two types of quenching for fluorescence: static quenching, which forms between fluorophores and a quencher, and dynamic quenching, which depends on temperature [35,36]. A higher diffusion coefficient and an increased quenching constant result from elevated temperatures. Based on the Stem-Volmer equation, the quenching mechanism and quenching constant were investigated [37-42].

$$\frac{F0}{F} = 1 + kq\tau 0[Q] = 1 + Ksv[Q] \quad (1)$$

Where F_0 and F are the fluorescence intensities before and after addition of the quencher, respectively, kq is the biomolecular quenching constant, τ_0 is the lifetime of the fluorophore in the absence of the quencher, $[Q]$ is the concentration of the quencher, and Ksv is the stem-Volmer quenching constant. As a result, the Ksv is found using linear regression of a plot of F0/F against [Q] using the equation above. According to Mohan *et al*. (2018), a linear Stern-Volmer plot often represents a single class of fluorophores that are all equally accessible to the quencher [11].

Analysis was done to determine whether β-ionone affected the intensity of BSA fluorescence. The fluorescence spectra of BSA with β-Ionone were documented in 300 to 550 nm, respectively. Tryptophan was the primary residue, and we saw that the fluorescence

intensity of BSA diminished as the β-Ionone concentration raised at 340 nm (Figure 1a), and we observed the slight red shift indicating the interaction of β-Ionone induced hydrophilicity to the protein fluorophore [43,44]. In the present study, Stern-Volmer plots observed interaction between β-Ionone and BSA at various temperatures was calculated by Stern-Volmer plots.

By using Stern-Volmer plots, the interaction between β-Ionone with BSA at different temperatures was analyzed (Figure 1b, 1c). The *Ksv* and *Kq* value for the β-Ionone with BSA was revealed in Table 1. The *Ksv* value declined upon increasing temperature. It is essential to associate the reduction in quenching constant with a decrease in the protein-ligand complex's stability as temperature rises. According to static quenching, the quenching constant (Ksv) tends to decrease as temperatures rise. The highest scatter collision quenching constant for dynamic collisions is 2.0×1010 $mol^{-1}s^{-1}$, a well-known fact [45,46]. Even so, the quenching constant (Kq) in the current work has a higher value of 1013, greater than 2.01010 $mol^{-1}s^{-1}$, indicating that a static quenching process may have occurred for the -ionone with BSA.

Table 1. Thermodynamic parameters of the β-Ionone with BSA interaction at several temperatures, as well as the Stern-Volmer quenching constant (Ksv) and binding constant (Kb).

	T	10^{5} K_{sv} (L mol^{-1})	10^{13} K_q (L mol^{-1})	n	ΔH (kJ mol^{-1})	ΔS (JK^{-1} mol^{-1})
Beta ionone	298	0.1336±0.00668	-0.989±0.0434	0.705±0.0470	-0.2664	-3.3426
	310	0.1144 ±0.0069	-1.124±0.038	0.797±0.0416		
	313	0.0644±0.0052	-2.812±0.0336	2.353±0.3841		

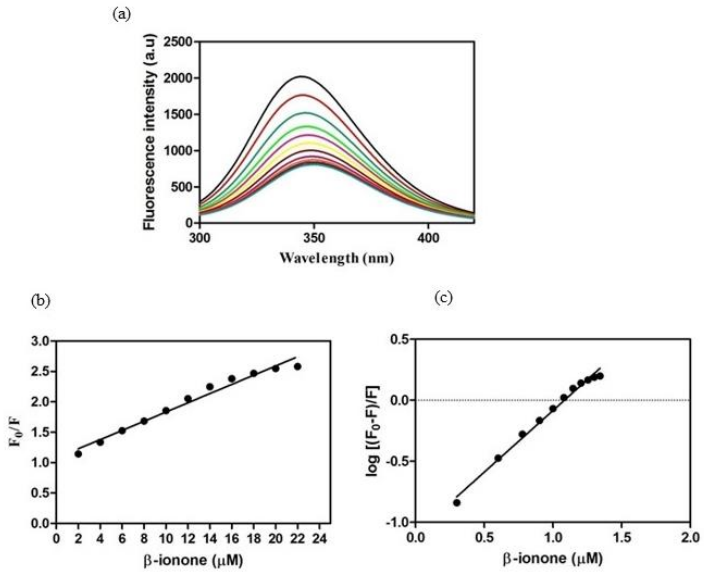

Figure 1. (a) Fluorescence emission spectra of BSA at different β-Ionone concentrations. The chemicals range in concentration from 0 to 10 μm, and Stern-Volmer graphs show how different concentrations of **(b)** β-Ionone BSA quench fluorescence—double logarithmic curve for **(c)** β-Ionone BSA fluorescence quenching.

3.2. Study of binding constant and binding sites.

The following equation was used to study the quenching process, such as the number of binding sites and binding constant:

$$log\ (F0 - F/F0)\ =\ -logKb\ +\ nlog[Q] \qquad (2)$$

Where n is the total number of binding sites shown in Table 1, and Kb is the binding constant. Examined was the binding constant of β-Ionone with BSA. The outcome clearly

shows that the binding number was close to one as the temperature increased and that the binding constant grew temperature-dependent [47,10].

3.3. Thermodynamics parameters of BSA with β-ionone.

Van der Waals, hydrophobic interaction, hydrogen bonding, and electrostatic interaction are some forces that interact with extremely small molecules and biomolecules. When analyzing the contact forces, thermodynamic factors, including the reaction's free energy changes (ΔG), entropy changes (ΔS), and enthalpy changes (ΔH) are crucial.

The enthalpy change *(ΔH)* and entropy *(ΔS)* can be calculated by Van't Hoff equation:

$$Ln\,Ka = -\Delta H/RT + \Delta S/R \quad [Q] \qquad (3)$$

Here, R is the gas factor, and Ka is the binding constant of the associated temperature. The Van't Hoff equation's slope was used to get the enthalpy change (ΔH). The following equation was used to

$$\Delta G = \Delta H - T\Delta S \qquad (4)$$

By using the linear second law of thermodynamics, the thermodynamic parameter was analyzed. To study the binding mode of BSA with β-Ionone, it is essential to examine the enthalpy-entropy relation. We studied temperature-dependent binding constant using three diverse temperatures without any structural degradation of BSA [48,10,49,46].

Table 1 displays the thermodynamic parameters such as *ΔH* and *ΔS* values for the interaction of β-Ionone with BSA. The negative *ΔH* and the negative *ΔS* indicate that the binding process of β-Ionone with BSA was spontaneous and the formation of β-Ionone and BSA complex was an exothermic reaction [50,51]. The outcome enables us to comprehend how hydrophobic forces and thermodynamic interaction relate and how hydrogen bonds are essential to the reaction.

3.4. Three-dimensional fluorescence spectra.

Three-dimensional fluorescence spectra are a prominent technique for studying conformational changes such as excitation wavelength, emission wavelength, and fluorescence intensity of proteins. In this study, the result shows 3D-fluorescence spectra of BSA alone and β-Ionone with BSA. The present data represents the fluorescence spectra of the typical Rayleigh scattering peak and emission peak of tryptophan tyrosine residues of BSA. The intensity spectra of fluorescence speak were decreased after interaction with β-Ionone, which signifies the conformational changes induced by β-Ionone (Figure 2). The BSA intensity was decreased by altering the peptide backbone and the amino acid residues of the protein; thereby, the conformational change is visualized [52].

3.5. Secondary structural analysis of β -ionone with BSA.

The circular dichroism spectrum is an insightful method for assessing the conformation alteration of subsidiary structures of protein interface with the ligand. Based on the shape of the spectral curve and also by positive and negative maxima, it gives details about the protein structure. The α-helix, β-turns, β-sheets, and random coil structures are thoroughly documented in the far-ultraviolet wavelength range of 200–250 nm, while the tertiary structure of proteins

is thoroughly documented in the near-UV range of 250–300 nm. By this result, we can understand the structural changes of BSA with β-Ionone [53].

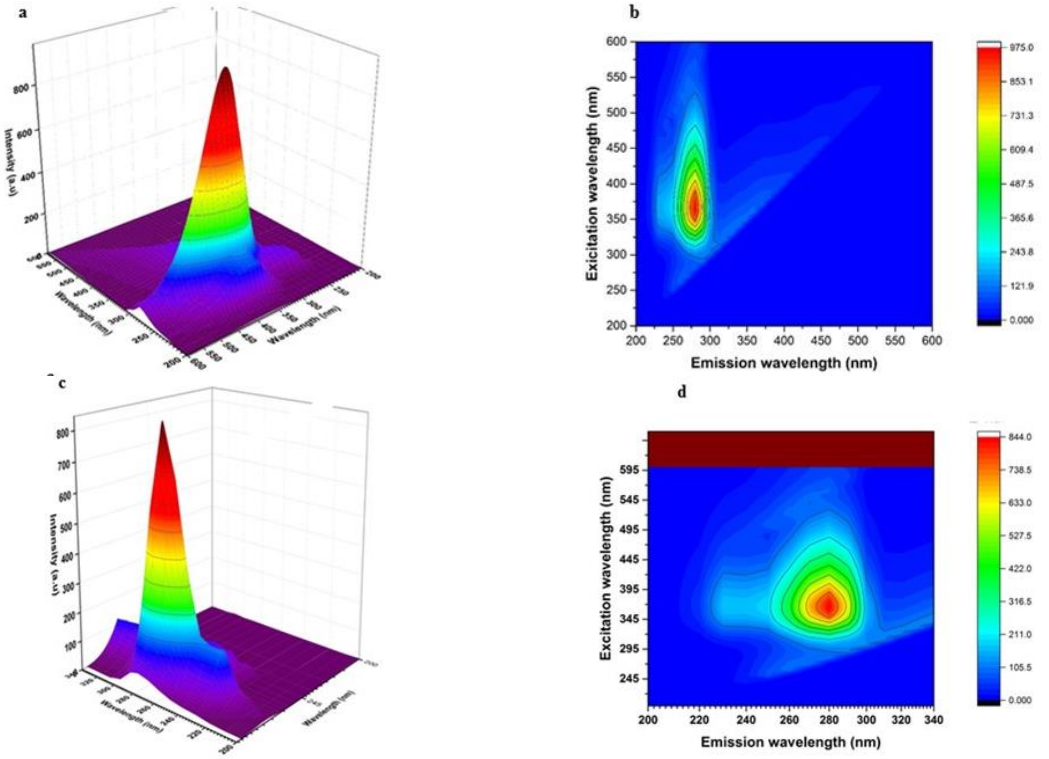

Figure 2. 3D fluorescence spectra and contour map of **(a,b)** BSA alone; **(c,d)** β-Ionone with the presence and absence of BSA.

Figure 3 shows that BSA with β-Ionone revealed two negative absorption minima at the UV region of 208 nm and 222 nm significantly, which contributes to the n → π* and π → π * transition in the α-helix representing the protein structure [48]. With the addition of BSA, the relative band intensity of the negative ellipticity reduced frequently, which proposed the conformational changes in the secondary structure of the protein. The secondary structures of BSA with the presence or absence of β-Ionone were examined with different ratios. The secondary structural components of the proteins experienced a crucial conformational shift due to the β -ionone interaction. The obtained result indicates that β-Ionone generated a variation in BSA's secondary structure, indicating that β-Ionone and BSA contact causes a conformational shift in the protein's secondary structure [46].

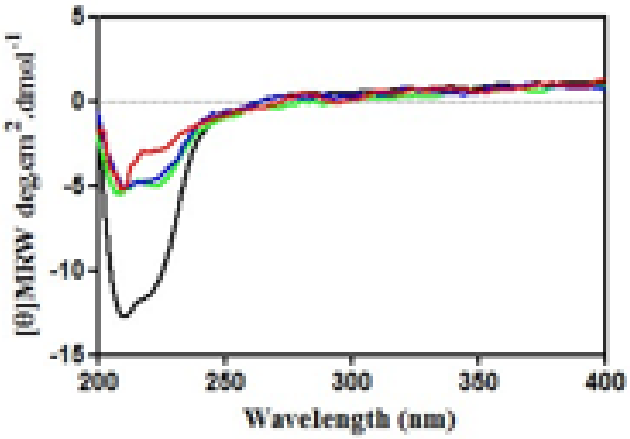

Figure 3. β-ionone's circular dichroism spectra with BSA. β-Ionone concentrations were found to be 1, 2, and 10 µm.

3.6. Molecular docking.

The molecular dockings were performed using the AutoDock. The binding energies between the BSA and HSA with β-Ionone were found to be -6.2 kcal/mol and -6.6 kcal/mol, respectively (Table 2). The interacting amino acids were visualized using the Discovery Studio software. The interacting amino acids of BSA with β-Ionone are TYR137, LYS136, LEU122, LEU115, PHE133, and TYR160 (Fig. 4a). The interacting amino acids of HSA with β-Ionone are ILE290, LEU219, LEU260, ALA291, ARG257, VAL241, LYS199, HIS242, and LEU238 (Fig. 4b).

Table 2. Docking score of the ligands using Autodock Software. Autodock Score interprets the binding affinity of the ligands.

Ligand	Auto dock-Score	Residue involved in interaction with (BSA)
Beta ionone	-6.2	TYR137, LYS136, LEU122, LEU115, PHE133,TYR160

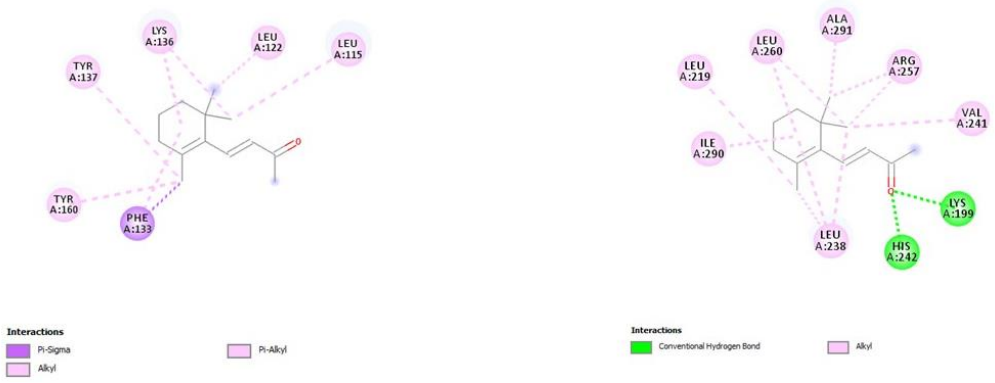

(a) **(b)**

Figure 4. Surrounding amino acids around beta-ionone with (a)BSA and (b) HSA.

3.7. Molecular dynamics simulations.

The RMSD, RMSF, and radius of gyration were analyzed for the BSA- β-Ionone and HSA- β-Ionone complexes after the simulation for 10ns. From the RMSD analysis, we observed a deviation between ~0.15 nm to ~0.65 nm in the BSA- β-Ionone complex (Figure 5a). On the other hand, the HSA- β-Ionone complex showed a deviation between ~0.15 nm to ~0.45 nm (Figure 5b). RMSF showed a similar fluctuation to that of the deviation observed in RMSD. The fluctuation of the BSA- β-Ionone complex reached up to ~0.65 nm, whereas the fluctuation of the HSA- β-Ionone complex reached up to ~0.4nm (Figure 5c, d). The deviation in the radius of gyration of the BSA- β-Ionone complex showed ~2.75 nm to ~2.88 nm, whereas the HSA- β-Ionone complex showed ~2.68 nm to ~2.76 nm (Figure 6a, b). These results show that the β-Ionone has better interaction and compactness with the BSA than the HSA.

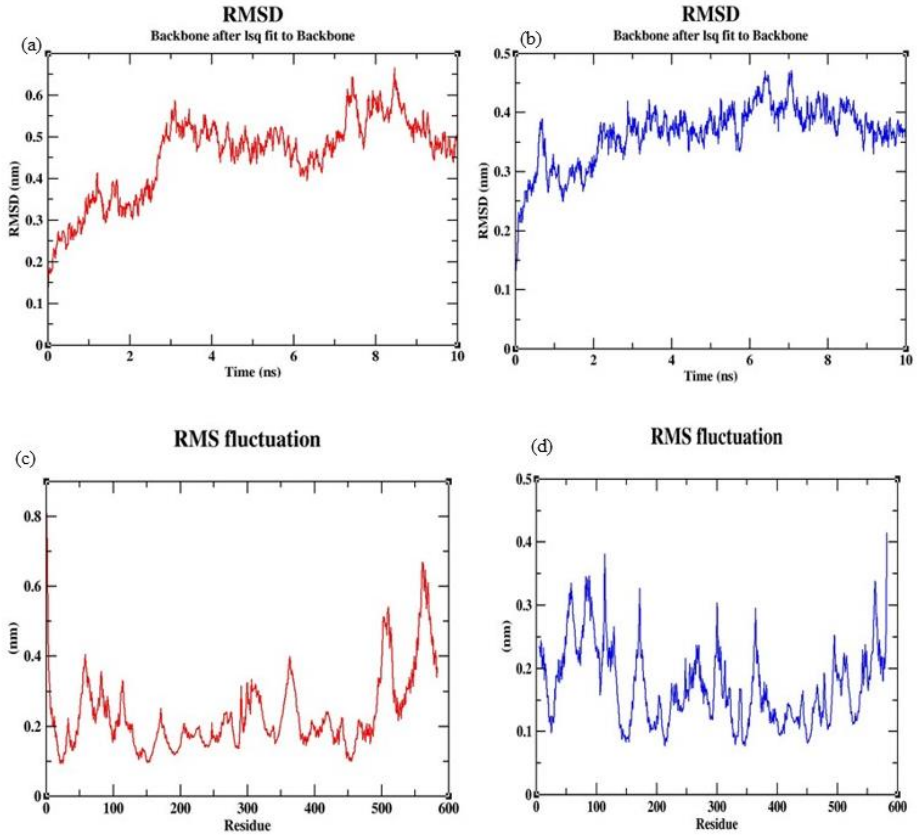

Figure 5. (a,b) Root Mean Square Deviation of the BSA-β-Ionone complex and HSA-β-Ionone complex; **(c,d)** Root Mean Square Fluctuation of the BSA-β-Ionone complex and HSA-β-Ionone complex

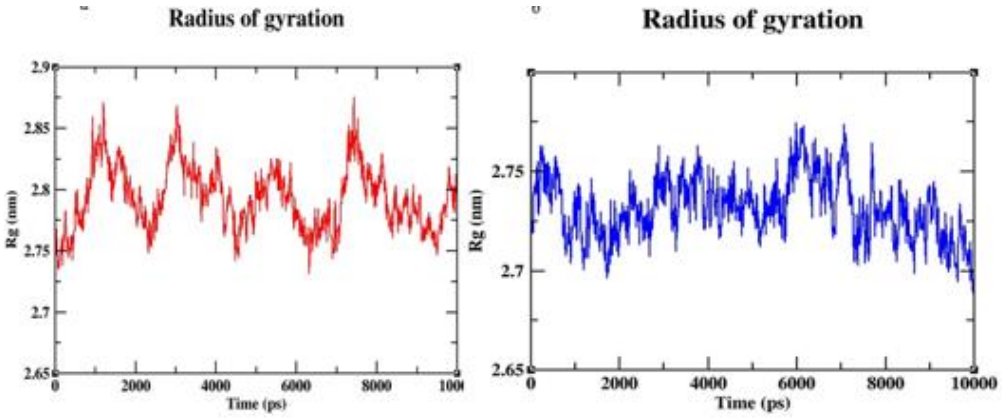

Figure 6. (a) The radius of gyration of the BSA-β-Ionone complex and (b) The radius of gyration of the HSA-β-Ionone complex.

3.8. Toxicity prediction.

The toxicity prediction for β-Ionone was achieved by ProTox and the pkCSM server. The ProTox tool reveals that the apocarotenoid is revealed as a Class 4 drug, and the LD50 score was 1620 mg/kg, correspondingly. As of the pkCSM tool, we recognized that β-Ionone does not possess any AMES toxicity. The toxicity investigation envisages no harsh, noxious effect of this ligand (Table 3).

Table 3. Toxicity analysis of the ligands using Protox and pkCSM servers.

Ligand	Protox Toxicity Class	Predicted LD50 (mg/kg)	AMES toxicity
Beta ionone	Class 4	1620	No

4. Conclusions

In summary, the mode of β-Ionone interacting with BSA was scrutinized through spectroscopic techniques. Experimental outcomes reveal that β-Ionone interacts with albumin protein and suppresses the fluorescence emission of albumin protein through the static quenching mechanism. The binding parameter of β-Ionone with BSA was due to entropy. The CD spectrum and 3D fluorescence spectra analysis established the configurational changes of BSA upon β-Ionone interaction. Furthermore, this binding mechanism was revealed with the help of a molecular docking study. In conclusion, β-Ionone would be efficiently adopted as a food additive as it affirms affinity with BSA. In futurity, this investigation will endow insight into the interaction of albumin protein with β-Ionone to unravel the transit and absorption of this food additive in serum.

Funding

The authors are grateful to VIT University management for their constant support. The authors are thankful to the VIT-Sophisticated Instrumentation Facility Laboratory, School of Advanced Sciences, Chemistry Division, for fluorescent spectroscopy, and we thank Dr. G. Jayaraman, School of Bioscience and Technology, VIT University, for the CD spectrum facility.

Acknowledgments

The authors are grateful to VIT University management for their constant support. The authors are thankful to the VIT-Sophisticated Instrumentation Facility Laboratory, School of Advanced Sciences, Chemistry Division, for fluorescent spectroscopy, and we thank Dr. G. Jayaraman, School of Bioscience and Technology, VIT University, for the CD spectrum facility.

Conflicts of Interest

All authors declare no competing interest.

References

1. Paparella, A.; Shaltiel-Harpaza, L.; Ibdah, M. β-Ionone: Its occurrence and biological function and metabolic engineering. *Plants.* **2021**, *10*, 754, https://doi.org/10.3390/plants10040754.
2. Simkin, A.J.; Underwood, B.A.; Auldridge, M.; Loucas, H.M.; Shibuya, K.; Schmelz, E.; Clark, D.G.; Klee, H.J., Circadian regulation of the PhCCD1 carotenoid cleavage dioxygenase controls emission of β-ionone, a fragrance volatile of petunia flowers. *Plant Physiology* **2014**, *136*, 3504–3514, https://doi.org/10.1104/pp.104.049718.
3. Han, Y.; Wang, H.; Wang, X.; Li, K.; Dong, M.; Li, Y.; Zhu, Q. Shang F. Mechanism of floral scent production in Osmanthus fragrans and the production and regulation of its key floral constituents, β-ionone and linalool. *Horticulture research.* **2019**, *6*, https://doi.org/10.1038/s41438-019-0189-4.
4. Ipte, P.R.; Sahoo, S.; Satpati, A.K. Spectro-electrochemistry of ciprofloxacin and probing its interaction with bovine serum albumin. B*ioelectrochemistry* **2019**, *130*, 107330, https://doi.org/10.1016/j.bioelechem.2019.107330.
5. Behera, S.; Mohanty, P.; Dash, P.P.; Mohapatra, P.; Shubhadarshinee, L.; Behura, R.; Barick, A.K.; Mohapatra, P.; Jali, B.R. Selective Binding of Bovine Serum Albumin (BSA): A Comprehensive Review. *Biointerface Res. Appl. Chem.* **2023**, *13*, 555, https://doi.org/10.33263/BRIAC136.555.
6. Akhuli, A.; Chakraborty, D.; Agrawal, A.K.; Sarkar, M. Probing the interaction of bovine serum albumin with copper nanoclusters: realization of binding pathway different from protein corona. *Langmuir*. **2021**, *37*, 1823-1837, https://doi.org/10.1021/acs.langmuir.0c03176.

7. Saha, D.; Ray, D.; Kumar, S.; Kohlbrecher, J; Aswal, V.K. Interaction of a bovine serum albumin (BSA) protein with mixed anionic–cationic surfactants and the resultant structure. *Soft Matter*. **2021**, *17*, 6972-6984, https://doi.org/10.1039/d1sm00264c.
8. Ansari, A. Decoding the binding interaction of steroidal pyridines with bovine serum albumin using spectroscopic and molecular docking techniques. *Steroids* **2023**, *192*, 109156, https://doi.org/10.1016/j.steroids.2022.109156.
9. Shahabadi, N.; Maghsudi, M.Z.; Kiani, M.; Pourfoulad, M. Multispectroscopic studies on the interaction of 2-tert-butylhydroquinone (TBHQ), a food additive, with bovine serum albumin. *Food Chemistry*. **2014**, *124*, 1063–1068, https://doi.org/10.1016/j.foodchem.2010.07.079.
10. Li, X.; Wang, G.; Chen, D; Lu, Y. β-Carotene and astaxanthin with human and bovine serum albumins. *Food Chemistry*. **2015**, *179*, 213–221, https://doi.org/10.1016/j.foodchem.2015.01.133.
11. Mohan, S.; Hemachandran, H.; Sneha, P.; George Priya Doss, C.; Godwin Christopher, J.; Jayaraman, G.; Ramamoorthy, S. Structural insights into the binding mode and conformational changes of BSA induced by bixin and crocin. *Journal of Biomolecular Structure and Dynamics* **2018**, *36*, 2085-2098, https://doi.org/10.1080/07391102.2017.1342565.
12. Paiva, P.H.C.; Coelho, Y.L.; da Silva, L.H.M.; Pinto, M.S.; Vidigal, M.C.T.; Pires, A.C.D.S. Influence of protein conformation and selected Hofmeister salts on bovine serum albumin/lutein complex formation. *Food chemistry*. **2020**, *305*,125463, https://doi.org/10.1016/j.foodchem.2019.125463.
13. Negrea, E.; Oancea, P.; Leonties, A.; Maria, U.A.; Avram, S.; Raducan, A. Spectroscopic studies on binding of ibuprofen and drotaverine with bovine serum albumin. *Journal of Photochemistry and Photobiology A: Chemistry* **2023**, *438*, 114512, https://doi.org/10.1016/j.jphotochem.2022.114512.
14. Narayan, S.; Rajagopalan, A.; Reddy, J.S.; Chadha, A. BSA binding to silica capped gold nanostructures: effect of surface cap and conjugation design on nanostructure–BSA interface. *RSC Advances* **2014**, *4*, 1412-1420, https://doi.org/10.1039/C3RA45887C.
15. Korkma, F.; Erdogan, D.A.; Özalp-Yaman, Ş. Interaction of a novel platinum drug with bovine serum albumin: FTIR and UV-Vis spectroscopy analysis. New *Journal of Chemistry* **2015**, *39*, 5676-5685, https://doi.org/10.1039/C5NJ00785B.
16. Zsila, P.; Molnár, J.; Deli. Analysis of binding interaction between the natural apocarotenoid bixin and human serum albumin by circular dichroism and fluorescence spectroscopy. *Chemistry and Biodiversity* **2005**, *2*, 758-72, https://doi.org/10.1002/cbdv.200590053.
17. Hridya, H.; Amrita, A.; Mohan. S.; Gopalakrishnan. M.; Dakshinamurthy, T.K.; Doss, G.P.; Siva, R. Functionality study of santalin as tyrosinase inhibitor: A potential depigmentation agent. *International Journal of Biological Macromolecules* **2016**, *86*, 383-389, https://doi.org/10.1016/j.ijbiomac.2016.01.098.
18. Manavi, A.; Ray, D.; Asal, V.K.; Bhattacharyya, J. Understanding the molecular interaction of BSA protein with antibiotic sulfa molecule (s) for novel drug development. *Journal of Molecular Structure* **2023**, *1287*, 135697, https://doi.org/10.1016/j.molstruc.2023.135697.
19. Liang, W.; Zhang, Z.; Zhu, Q.; Han, Z.; Huang, C.; Liang, X.; Yang, M. Molecular interactions between bovine serum albumin (BSA) and trihalophenol: Insights from spectroscopic, calorimetric and molecular modeling studies. *Spectrochimica Acta Part A: Molecular and Biomolecular Spectroscopy* **2023**, *287*, 122054, https://doi.org/10.1016/j.saa.2022.122054.
20. Peng, M.; Wang, Y.; Wu, C.; Cai, X.; Wu, Y.; Du, E.; Zheng, L.; Fu, J. Investigating sulfonamides-Human serum albumin interactions: A comprehensive approach using multi-spectroscopy, DFT calculations, and molecular docking. *Biochemical and Biophysical Research Communications* **2023**, *683*, 149108, https://doi.org/10.1016/j.bbrc.2023.10.040.
21. Sekar, G,; Haldar, M.; Kumar, D.T.; Doss, C.G.P.; Mukherjee, A.; Chandrasekaran, N. Exploring the interaction between iron oxide nanoparticles (IONPs) and human serum albumin (HSA): spectroscopic and docking studies. *Journal of Molecular Liquids* **2017**, *241*, 793-800, https://doi.org/10.1016/j.molliq.2017.06.093.
22. Peng, M.; Xu, Y.; Wu, Y.; Cai, X.; Zhang, W.; Zheng, L.; Du, E.; Fu, J. Binding Affinity and Mechanism of Six PFAS with Human Serum Albumin: Insights from Multi-Spectroscopy, DFT and Molecular Dynamics Approaches. *Toxics* **2024**, *12*, 43, https://doi.org/10.3390/toxics12010043.
23. Han, W.; Yang, Y.; Zhang, H.; Qiao, H.; Zhang, Y.; Zhang, Z.; Wang, J. Interaction of different chloro-substituted phenylurea herbicides (diuron and chlortoluron) with bovine serum albumin: Insights from multispectral study. *Spectrochimica Acta Part A: Molecular and Biomolecular Spectroscopy* **2024**, 124338, https://doi.org/10.1016/j.saa.2024.124338.

24. Bujacz, A. Structures of bovine, equine and leporine serum albumin. Acta Crystallographica Section D: *Biological Crystallography* **2012**, *68*, 1278-1289, https://doi.org/10.1107/S0907444912027047.
25. Janani, S.; Rajagopal, H.; Sakthivel, S.; Kadaikunnan, S.; Abbas, G.; Muthu, S.; Comparison of experimental and theoretical spectral groups, electronic properties, topological, and molecular docking investigations of 1-N-Cbz-piperidine-4-carboxylic acid-Potential Cancer drug. *Journal of Molecular Structure* **2023**, *1289*, 135832, https://doi.org/10.1016/j.molstruc.2023.135832.
26. Gatfaoui, S.; Issaoui, N.; Kazachenko, A.S.; Al-Dossary, O.M.; Roisnel, T.; Marouani, H. Synthesis, characterization and identification of inhibitory activity on the main protease of COVID-19 by molecular docking strategy of (4-oxo-piperidinium ethylene acetal) trioxonitrate. *Journal of King Saud University-Science* **2023**, *35*, 102758, https://doi.org/10.1016/j.jksus.2023.102758.
27. Kalita, G.; Sarmah, S.; Roy, A.S.; Chatterjee, P.N. Synthesis of 2, 2-disubstituted-2 H-1-benzopyrans using tetraphenylethylene-based heterogeneous acidic organocatalyst and the evaluation of their binding interaction with human serum albumin. *Journal of Heterocyclic Chemistry* **2023**, *60*, 297-317, https://doi.org/10.1002/jhet.4582.
28. Umadevan, I.; Rajasekaran, R.; Bennet, M.A.; Rajmohan, V.; Vetrivelan, V.; Sankar, K.; Raja, M. Synthesis, spectroscopic, chemical reactivity, topology analysis and molecular docking study of ethyl 5-hydroxy-2-thioxo-4-(p-tolyl)-6-(trifluoromethyl) hexahydropyrimidine-5-carboxylate. *Heliyon* **2024**, *10*, e224588, https://doi.org/10.1016/j.heliyon.2024.e24588.
29. Pettersen, E.F.; Goddard, T.D.; Huang, C.C.; Couch, G.S.; Greenblatt DM, Meng EC, Ferrin TE. UCSF Chimera—a visualization system for exploratory research and analysis. *Journal of Computational Chemistry* **2004**, *25*, 1605-1612, https://doi.org/10.1002/jcc.20084.
30. Reeda, V.J.; Jothy, V.B. Vibrational spectroscopic, quantum computational (DFT), reactivity (ELF, LOL and Fukui), molecular docking studies and molecular dynamic simulation on (6-methoxy-2-oxo-2H-chromen-4-yl) methyl morpholine-4-carbodithioate. *Journal of Molecular Liquids* **2023**, *371*, 121147, https://doi.org/10.1016/j.molliq.2022.121147.
31. Jiang, S.L.; Wang, W.J.; Hu, Z.Y.; Zhang, R.J.; Shi, J.H. Comprehending the intermolecular interaction of JAK inhibitor fedratinib with bovine serum albumin (BSA)/human alpha-1-acid glycoprotein (HAG): Multispectral methodologies and molecular simulation. *Spectrochimica Acta Part A: Molecular and Biomolecular Spectroscopy* **2024**, *304*, 123277, https://doi.org/10.1016/j.saa.2023.123277.
32. Drwal, M.N.; Banerjee, P.; Dunkel, M.; Wettig, M.R.; Preissner, R. ProTox: a web server for the in silico prediction of rodent oral toxicity. *Nucleic acids research* **2014**, *42*, W53-W58, https://doi.org/10.1093/nar/gku401.
33. Pires. D.E.; Blundell, T.L.; Ascher, D.B. pkCSM: predicting small-molecule pharmacokinetic and toxicity properties using graph-based signatures. *Journal of Medicinal Chemistry* **2015**, *58*, 4066-4072, https://doi.org/10.1021/acs.jmedchem.5b00104.
34. Wu, C.; Wang, Y.; Cai, X.; Wu, Y.; Du, E.; Zheng, L.; Peng, M. Investigating haloacetic acids-human serum albumin interactions: A comprehensive approach using multi-spectroscopy, DFT calculations, and molecular docking. *Journal of Molecular Structure* **2024**, *1299*, 137143, https://doi.org/10.1016/j.molstruc.2023.137143.
35. Zhang, G.; Wang, A.; Jiang, T.; Guo, J. Interaction of the irisflorentin with bovine serum albumin: a fluorescence quenching study. *Journal of Molecular Structure* **2008**, *891*, 93-97, https://doi.org/10.1016/j.molstruc.2008.03.002.
36. Li, X.; Chen, D.; Wang, G.; Lu, Y. Study of interaction between human serum albumin and three antioxidants: Ascorbic acid, α-tocopherol, and proanthocyanidins. *European Journal of Medicinal Chemistry* **2013**, *70*, 22-36, https://doi.org/10.1016/j.ejmech.2013.09.033.
37. Sarwar, T.; Rehman, S.U.; Husain, M.A.; Ishqi, H.M.; Tabish, M. Interaction of coumarin with calf thymus DNA: deciphering the mode of binding by in vitro studies. *International Journal of Biological Macromolecules.* **2015**, *73*, 9-16, https://doi.org/10.1016/j.ijbiomac.2014.10.017.
38. Lakowicz, J.R. ed., **2006**. Principles of fluorescence spectroscopy. Boston, MA: springer US, https://doi.org/10.1007/978-0-387-46312-4.
39. Kim, D.; Park, J.; Kim, J.; Han, C.; Yoon, J.; Kim, N.; Seo, J.; Lee, C. Flavonoids as mushroom tyrosinase inhibitors: a fluorescence quenching study. *Journal of Agricultural and Food Chemistry* **2006**, *54*, 935-941, https://doi.org/10.1021/jf0521855.

40. Tan, C.; Atas, E.; Müller, J.G.; Pinto, M.R.; Kleiman, V.D.; Schanze, K.S. Amplified quenching of a conjugated polyelectrolyte by cyanine dyes. *Journal of the American Chemical Society* **2004**, *126*, 13685-13694, https://doi.org/10.1021/ja046856b.
41. Lazniewska, J.; Agostino, M.; Hickey, S.M.; Parkinson-Lawrence, E.; Stagni, S.; Massi, M.; Brooks, D.A.; Plush, S.E. Spectroscopic and molecular docking study of the interaction between neutral Re (I) tetrazolate complexes and bovine serum albumin. *Chemistry–A European Journal* **2021**, *27*, 11406-11417, https://doi.org/10.1002/chem.202101307.
42. Göktürk, T.; Sakallı Çetin, E.; Hökelek, T.; Pekel, H.; Şensoy, O.; Aksu, E.N.; Güp, R. Synthesis, structural investigations, DNA/BSA interactions, molecular docking studies, and anticancer activity of a new 1, 4-disubstituted 1, 2, 3-triazole derivative. *ACS omega* **2023**, *8*, 31839-31856, https://doi.org/10.1021/acsomega.3c03355.
43. Malde, A.K.; Zuo, L.; Breeze, M.; Stroet, M.; Poger, D.; Nair, P.C.; Oostenbrink, C.; Mark, A.E. An automated force field topology builder (ATB) and repository: version 1.0. *Journal of Chemical Theory and Computation* **2011**, *7*, 4026-4037, https://doi.org/10.1021/ct200196m.
44. Szymaszek, P.; Fiedor, P.; Chachaj-Brekiesz, A.; Tyszka-Czochara, M.; Świergosz, T.; Ortyl, J. Molecular interactions of bovine serum albumin (BSA) with pyridine derivatives as candidates for non-covalent protein probes: a spectroscopic investigation. *Journal of Molecular Liquids* **2022**, *347*, 118262, https://doi.org/10.1016/j.molliq.2021.118262.
45. Chaturvedi, S.K.; Ahmad, E.; Khan, J.M.; Alam, P.; Ishtikhar, M.; Khan, R.H. Elucidating the interaction of limonene with bovine serum albumin: a multi-technique approach. *Molecular BioSystems* **2015**, *11*, 307-316, https://doi.org/10.1039/c4mb00548a.
46. Ishtikhar, M.; Khan, S.; Badr, G.; Osama Mohamed, A.; Khan, R.H. Interaction of the 5-fluorouracil analog 5-fluoro-2'-deoxyuridine with 'N' and 'B' isoforms of human serum albumin: a spectroscopic and calorimetric study. *Molecular Biosystems* **2014**, *10*, 2954-64, https://doi.org/10.1039/c4mb00306c.
47. Hu, Y.J.; Liu, Y; Wang, J.B.; Xiao, X.H.; Qu, S.S. Study of the interaction between monoammonium glycyrrhizinate and bovine serum albumin. *Journal of Pharmaceutical and Biomedical Analysis.* **2014**, *36*, 915-919, https://doi.org/10.1016/j.jpba.2004.08.021.
48. Han, X.L.; Mei, P.; Liu, Y; Xiao, Q.; Jiang, F.L.; Li, R. Binding interaction of quinclorac with bovine serum albumin: a biophysical study. Spectrochimica Acta Part A: *Molecular and Biomolecular Spectroscopy.* **2009**, *74*, 781-787, https://doi.org/10.1016/j.saa.2009.08.018.
49. Anantharaman, A; Hemachandran, H.; Priya, R.R.; Sankari, M.; Gopalakrishnan, M.; Palanisami, N.; Siva, R. Inhibitory effect of apocarotenoids on the activity of tyrosinase: multi-spectroscopic and docking studies. *Journal of Bioscience and Bioengineering* **2016**, *121*, 13-20, https://doi.org/10.1016/j.jbiosc.2015.05.007.
50. Ross, P.D.; Subramanian, S. Thermodynamics of protein association reactions: forces contributing to stability. *Biochemistry.* **1981**, *20*, 3096-3102, https://doi.org/10.1021/bi00514a017.
51. Li, X.F.; Yang, Y.Q.; Li, Y.X.; Yang, H.X.; Zhao, W.F.; Meng, X.R. Synthesis, crystal structure, and BSA binding studies of new Co (II) and Ni (II) complexes of 2-(hydroxymethyl)-1H-imidazole-4, 5-dicarboxylate. *Inorganica Chimica Acta* 2020, *505*, 119469, https://doi.org/10.1016/j.ica.2020.119469.
52. Makarska-Bialokoz, M. Analysis of the binding interaction in uric acid-Human hemoglobin system by spectroscopic techniques. *Spectrochim. Acta - A: Mol. Biomol. Spectrosc.* **2017**, *178*, 47-54, https://doi.org/10.1016/j.saa.2017.01.063.
53. Ranjbar, B.; Gill, P. Circular Dichroism Techniques: Biomolecular and Nanostructural Analyses- A Review. *Chem. Biol. Drug Des.* **2009**, *74*, 101-120, https://doi.org/10.1111/j.1747-0285.2009.00847.x.